Heat Transfer in Flow Boiling Conditions for Swirl Tube Elements Customizing the ANSYS Software

M. Dalla Palma, P. Zaccaria

Consorzio RFX, Associazione EURATOM - ENEA sulla Fusione

Corso Stati Uniti 4, I-35127, Area della Ricerca del CNR, Padova, Italy

Abstract

A heat transfer model with water coolant in flow boiling conditions for swirl tube elements is simulated customizing a programmable routine and relinking the ANSYS code.

The standard ANSYS features calculate the film coefficient for forced convection conditions in the single-phase flow without possibility of take into account flow boiling conditions.

The heat transfer coefficient is redefined in a general way customizing ANSYS by a user programmable routine to simulate the actual heat transfer in forced convection and flow boiling conditions. The modified routine is called for each iteration, once per element, and during each sub-step of each load-step. The heat transfer coefficient is calculated as a function of heat flux, surface and coolant temperatures, water saturation curve, fluid dynamic properties of coolant, twist tape pitch, and location.

A special function is implemented in the customized routine to reduce significantly the number of solution iterations. This function mitigates the heat flux instabilities due to nucleate boiling in the near-wall surface elements.

The customized ANSYS code is used to carry out thermo-hydraulic and thermo-structural analyses for the design of high heat flux components of the neutral beam injector for the international thermonuclear experimental reactor ITER.

Introduction

The standard ANSYS features calculate the film coefficient for forced convection conditions in single-phase flow. These features allow the generation of non-linear parametric models in which the film coefficient is defined as a material property that varies with fluid dynamic properties of coolant, temperature, and location.

In this way the implementation of the Lopina-Bergles correlation has been carried out for the film coefficient calculation for forced convection conditions in single phase flow. Modifications of the film coefficient can be considered to take into account the presence of twist tape in the swirl tube elements (STEs) [1].

Heat transfer in flow boiling conditions is foreseen in STEs for application in active cooled high heat flux components to take advantage of increased heat transfer coefficient. The flow boiling heat transfer for water coolant in swirl tube elements is simulated compiling and relinking a user programmable routine in the code.

The customized ANSYS code is used to carry out thermo-hydraulic and thermo-structural analyses for the design of active cooled high heat flux components of the neutral beam injector (NBI) for ITER international thermonuclear experimental reactor. An accelerated 1 MeV ion beam (40 MW accelerated negative beam power) entering the beam line components is only partially converted into the neutral beam delivered to ITER plasma (16.7 MW neutral beam power). The remaining part is deposited onto the beam line components and exhausted by the NBI cooling system [2]. The peak power density on the elements can reach values up to 25 MW/m^2, which essentially forces the use of water coolant in nucleate boiling conditions [1]. The code customization and the main results of the thermo-hydraulic and thermo-structural analyses of the neutralizer leading edge elements (LEEs) are presented in this work.

Mechanisms of Heat Transfer

Heat exchange in flow boiling conditions means the boiling phenomenon of a fluid in forced convection flow regime. Two main mechanisms of heat exchange can be identified during the flow boiling conditions:

1) convective boiling,
2) nucleate boiling.

The nucleate boiling (2) is present only if the heat flux exceeds the limit value for the bubbles nucleation (onset of nucleate boiling) and it occurs when the thermal resistance of the liquid boundary layer doesn't allow heat exchange by convection, then the over-heating of the liquid near the wall surface is sufficient to start-up the bubbles nucleation. The heat transfer occurs predominantly by latent heat transport in the vapor phase that grows at the wall surface. The heat transfer coefficient is predominantly function of the heat flux and pressure, in spite of the fluid dynamic parameters as flow-rate and vapor quality.

The convective boiling mechanism (1) occurs when the thermal resistance in the liquid boundary layer is less then one in the nucleate boiling and the over-heating of the near-wall liquid is insufficient to start-up the bubbles nucleation. The heat transfer occurs due to conduction and convection mechanisms in the liquid layer and due to the evaporation at the interface or in the liquid bulk. The heat transfer is predominantly function of the flow characteristics, as flow-rate, quality, in spite of heat flux and temperature.

Boiling Process in the Tube

The coolant flows in the tube exchanging heat with the wall that is heated from the outer surface of the tube. The fluid would be under-cooled at the inlet, then the heat transfer would happen by single-phase convection. The boiling in the under-cooled liquid occurs when the temperature of the liquid near the heated surface exceeds the boiling start-up temperature and then the vapor bubbles transport heat in the liquid bulk. This process (boiling in the under-cooled liquid) increases the liquid temperature along the flow direction and the generated turbulence increases the heat transfer coefficient.

The convective boiling mechanism (1) occurs if the heat flux is insufficient to start-up the bubbles nucleation. The heat transfer coefficient rises approximately proportionally with the vapor quality after the saturation is reached. The nucleate boiling mechanism (2) starts as far as the heat flux is high. In general the two regimes are co-existing.

The liquid layer diminishes as the heat flux increases, the boiling proceeds, and a critical state is reached when the film is completely evaporated leaving dry the wall surface. The flow-rate shall be high enough to prevent the critical heat flux arising. The net generation of vapor with increase in the quality occurs only when the vapor generated exceeds the absorbed. The bulk temperature rises up to saturation and then it decreases due to the pressure drop along the flow direction.

Heat Transfer and Thermo-hydraulic Models

The models implemented in the ANSYS customized codes are expressed by the following conservative correlations [3, 4].

Forced Convection Coefficient

The film coefficient is calculated in the ANSYS standard features with Lopina-Bergles correlation for forced convection conditions in the single-phase flow in the presence of the twist tape [5], corrected according to reference [6]:

$$q_t(T_i) = \alpha_t \cdot (T_i - T_f)$$

$$\alpha_t = Nu_t \cdot \lambda / D_h \qquad \text{with} \qquad Nu_t = 0.0343 \cdot (1+k^2)^{0.4} \cdot Re^{0.8} \cdot Pr^{0.33}$$

The convection coefficient is split in the product of to coefficients:

$$\alpha_t = C_1 \cdot C_2$$

The terms responsible of the geometric characteristics and the flow-rate are collected in the multiplier factor:

$$C_1 = \frac{0.0343}{D_h} \cdot \left(1 + k^2\right)^{0.4} \cdot \left(\frac{4 \cdot \dot{m}}{P_{wet}}\right)^{0.8}$$

where $\dot{m}$ is the coolant flow-rate,

P_{wet} is the wetted perimeter.

C_1 is calculated after the definition of the input parameters. A second coefficient considers the dependence of the thermo-physical properties on temperature:

$$C_2 = \lambda \cdot (1/\mu)^{0.8} \cdot Pr^{0.33}$$

with $\mu = \mu(T_f)$ dynamic viscosity,

$\lambda = \lambda(T_f)$ thermal conductivity,

$c = c(T_f)$ heat capacity at constant pressure,

$Pr = \frac{c(T_f) \cdot \mu(T_f)}{\lambda(T_f)} = Pr(T_f)$ is the Prandtl's number.

The C_2 coefficient is plotted versus temperature to define a polynomial function that is introduced in ANSYS as a material property with linear, quadratic, cubic, and quartic terms.

Flow Boiling Model for STEs

The formulation of the global heat transfer coefficient is based on the classical approach of combining the Lopina-Bergles equation for single-phase flow in the presence of the twist tape [5], with the Thom equation for boiling curve correlation [7] and Kutateladze technique for heat flux in fully developed boiling [8]. The heat transfer coefficient is calculated as a function of heat flux, coolant pressure, water saturation curve, twist tape pitch, cooling channel geometry, inner wall channel temperature, and fluid dynamic parameters that vary with temperature.

The following section examines the relations used to carry out the thermo-hydraulic assessment and the formulae implemented in the ANSYS customized routine to calculate the local heat transfer coefficient in flow boiling conditions.

Critical Heat Flux

The critical heat flux (CHF) is obtained by the generalized correlation for swirl tubes [1] developed by Yagov that is selected for simplicity of calculation and extended verification against a wide experimental database [9]:

$$CHF = 3.4 \cdot \eta_v^{0.291} \ [MW/m^2]$$

with $\eta_v = g_n/g_0 = k^2 \cdot v^2/(g \cdot D_h/2)$ and $k = \pi \cdot D_h/t_{tt}$

where v is the water axial velocity,

D_h is the inner duct diameter,

g is the gravity acceleration,

t_{tt} is the twist tape pitch,

k is the swirl ratio.

Verifications have been performed utilizing the modified Tong 75 correlation according to the CEA formulation [10], and good agreement is found.

The flow-rate necessary to exhaust the heat flux is valuated during the pre-processing of the thermal-hydraulic analyses considering appropriate values of the above parameters; in particular the twist tape pitch is defined.

Pressure Drop in STEs

An expression based on Darcy's formula [11] is used:

$$\Delta P_{tt} = \xi_{tt} \cdot (\rho \cdot v^2/2) \cdot (L_{tt}/D_h)$$

where ρ is the water mass density at the tube inlet

L_{tt} is the tube axial length

ξ_{tt} is the friction coefficient.

ξ_{tt} is calculated during the thermal-hydraulic analyses activating the data table for the fluid material with reference to several temperatures and Reynolds's numbers in the form:

$$\xi_{tt} = 7.5 \cdot k^{0.406} \cdot \varsigma_c \quad \text{with} \quad \varsigma_c = 0.358/Re^{0.25} \quad \text{and} \quad Re = v \cdot D_h/\nu_0$$

where ν_0 is the cinematic water viscosity at the tube inlet.

The effect of vapor-fluid mixture in the nucleate boiling zone close to the tube wall [3, 4] is taken into account.

Heat Transfer Coefficient

The classical approach of combining the Lopina-Bergles equation for single-phase flow with the Thom equation [7] for fully developed boiling through the Bergles-Rohsenow interpolation [12] in the nucleate boiling region is utilized:

1) forced convection conditions in the single phase flow with the Lopina-Bergles correlation for the heat transfer coefficient in the presence of the twist tape [5], corrected according to reference [6]:

$$q_t(T_i) = \alpha_t \cdot (T_i - T_f)$$

$$\alpha_t = Nu_t \cdot \lambda/D_h \quad \text{with} \quad Nu_t = 0.0343 \cdot (1+k^2)^{0.4} \cdot Re^{0.8} \cdot Pr^{0.33} \cdot (\mu/\mu_w)^{0.14}$$

where μ is the water local dynamic viscosity in the bulk,

μ_w is the water local dynamic viscosity at the tube inner wall flow;

2) surface boiling conditions with the boiling curve correlation in the Thom form [7], corrected according to reference [6]:

$$q_s(T_i) = A\cdot(T_i - T_s)^{2.8} \qquad \text{with} \qquad A = 160\cdot\exp(P_f/3.1)\ [W/(m^2\cdot {}^oC^{2.8})]$$

where P_f is the coolant flow pressure in the tube cross-section [MPa],

T_i is the temperature at the tube inner wall surface,

T_f is the bulk water average temperature,

T_s is the water saturation temperature at pressure P_f.

Water saturation curve approximation in the range of 0.1 MPa ÷ 2.0 MPa is used [13].

The heat flux exhaust into the coolant under conditions of surface boiling at the inner pipe walls is determined by the Kutateladze technique [8] as shown in Figure 1 [6]:

$$q_i(T_i) = q_t(T_i) + q_s(T_i) - q_s(T_{si})$$

where T_{si} is the boiling start-up temperature at the surface, exceeding the saturation temperature because of an overheating of the near-wall saturated water layer. T_{si} is derived on the basis of Bergles-Rohsenow correlation from the equation:

$$\alpha_t\cdot(T_{si} - T_f) = 15500\cdot P_f^{1.156}\cdot[1.8\cdot(T_{si} - T_s)]^n \qquad \text{where} \qquad n = 2.046/P_f^{0.0234}$$

Three regions of heat transfer conditions can occur in the tube channel (Figure 1):

A. single-phase turbulent coolant flow region;

B. turbulent flow with surface boiling;

C. region of heat transfer with boiling of the saturated coolant flow.

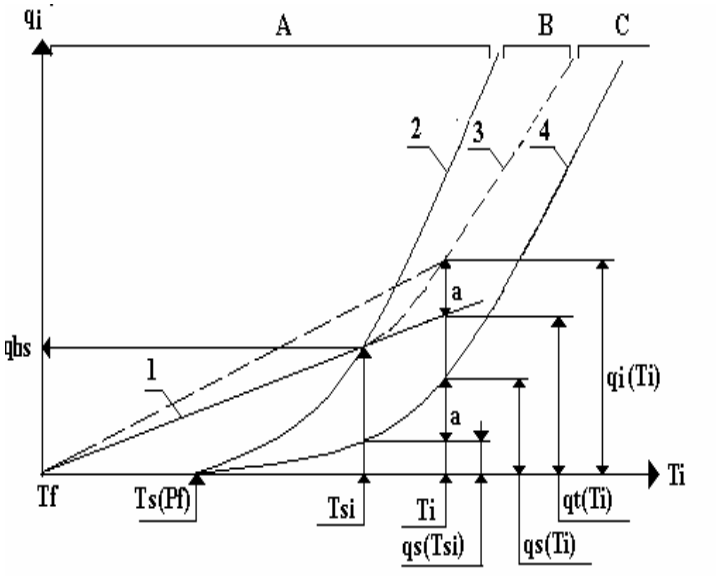

Figure 1. Regions of heat transfer conditions in the tube channel [6], $q_i(T_i)$ is heat flux. The regions are divided by the boundaries: 1) turbulent heat transfer boundary, 2) boundary of the surface boiling start-up, 3) boiling curve approximation in the forced coolant flow, 4) boiling curve for the saturated coolant flow.

The local heat transfer coefficient is calculated in each iteration, once per element, and during each sub-step of each load-step with the correlation:

$$\alpha_i = \begin{cases} \alpha_t & \text{for } T_i \le T_{si} \\ \alpha_t + A\cdot[(T_i - T_s)^{2.8} - (T_{si} - T_s)^{2.8}]/(T_i - T_f) & \text{for } T_i > T_{si} \end{cases}$$

Restrictions Concerning Cooling Conditions

The following hypotheses are to be satisfied because of the analytical model, matches on experimental data, well simulates the heat transfer phenomenon in flow boiling conditions [6]:

A. no bulk boiling in coolant flow, i.e. water mass-average temperature doesn't exceed saturation point at the tube exit;
B. stable heat removal in each tube cross-section, i.e. heat flux at the tube inner (cooling channel) surface doesn't exceed critical value.

Nucleate Boiling Instabilities

As considered in a previously section, the fluid would be under-cooled at the inlet, and the heat transfer would happen by single-phase convection. The nucleate boiling (2) is present only if the heat flux exceeds the limit value for the bubbles nucleation, then the over-heating of the liquid near the wall surface is sufficient to start-up the bubbles nucleation. The heat transfer is high due to the transport of latent heat in the vapor phase that grows at the wall surface. If the heat flux is insufficient to sustain this condition, the inner tube wall temperature decreases, the heat flux decreases and the nucleate boiling condition would not be satisfied (heat transfer by convective boiling mechanism 1). The reduced heat flux increases the wall temperature, and then the heat flux rises and the nucleate boiling condition would be satisfied with bubbles nucleation.

These variations in the prevalent mechanism of heat transfer are observed as instabilities in the simulation of the phenomena during the solution process between an iteration and the previous one of the thermo-hydraulic analyses. For this reason a special damping function is looked for to stabilize the heat transfer phenomena at the inner wall surface. The fluctuations are mitigates by means of the special function modifying the exchanged heat fluxes at two subsequent iterations. The motive-force of the exchanged heat flux, the difference between the inner wall tube temperature and the bulk temperature, is modified by the special function calculating the mean value of wall temperature between the current iteration and the previous one for each surface element. The effect of this special function called by the customized routine is to reduce significantly, at least one order of magnitude, the number of iterations to convergence.

User Programmable Routine Customization

The calculation of the heat transfer coefficient in flow boiling conditions in thermo-hydraulic analyses is carried out compiling and relinking the user programmable routine "usrsurf116" in the ANSYS code. The surface elements of the model "surf152" call this routine indirectly and the convection surface information is changed applying the formulae introduced in previous sections of this work. The call to get the standard ANSYS input convection surfaces is made just before entering this routine, so this information is available to be modified. The heat transfer coefficient is function of heat flux, surface and coolant temperatures, water saturation curve [13], fluid dynamic properties of coolant, twist tape pitch, and location, and it is calculated during each equilibrium iteration and during each sub-step of each load-step for each element. The extra nodes of "surf152" surface elements must be the same of the "fluid116" bulk elements to allow passing of information. The element types used in the model are described in the next section.

The properties and variables of the model are passed through the formal arguments of the routine and other quantities are brought in by "getv116" and "ndspgt" routines. The output argument of "getv116" routine named omega of fluid node, is utilized to pass the twist tape pitch (in the form of angular velocity $v\cdot 2\cdot\pi\cdot/t_{tt}$

with v = 10 m/s). Omega of fluid node is defined by the real constant that means the angular velocity associated with nodes of elements “fluid116”.

An iterative process is implemented in the customized routine to derive the exchanged heat flux and the boiling start-up temperature at each node on the basis of Bergles-Rohsenow correlation described in a previous section of this work.

The damping function is called by the customized routine to reduce significantly, at least one order of magnitude, the number of solution iterations. This function is based on the comprehension of the boiling physical phenomenon: the fluctuations in the exchanged heat flux are damped calculating the geometric mean of the inner wall surface temperature at two subsequent iterations for each element. The function mitigates the instabilities due to nucleate boiling in the near-wall surface elements and allows a faster convergence.

An output file is generated by the customized routine to record the heat transfer coefficients with and without flow boiling contribution, and the thermo-physical properties of fluid and surface elements where nucleate boiling occurs. These data are verified with analytical models but they are left out because not in the aims of this work.

Thermo-hydraulic and Thermo-structural Nonlinear Analyses of the LEEs

Calculations of thermo-hydraulic and thermo-mechanical design parameters of the beam line high heat flux components for the ITER neutral beam injector are performed by means of the customized ANSYS code. Thermo-hydraulic and thermo-mechanical analyses of the neutralizer LEEs with STEs are explained in this work.

The analyses are carried out with reference to NBI ITER operating conditions [1, 2] and applying the map of power densities (PDs) obtained by optic code simulations [17]. The geometry of the LEEs is adjusted to reduce the bending effect in the tube thickness. The breakdowns pause is diminished from 50-100 ms to 30 ms to decrease the material temperature range during breakdowns and then to increase the fatigue life in the plasma exposed region.

The upstream faces of the five panels of the NBI neutralizer are protected by the same number of LEEs. The LEE applied on the centre panel can experience a maximum frontal PD of 22 MW/m^2, 21.5 MW/m^2 of which are electrons PD and the other 0.5 MW/m^2 are ions PD. The analyses exposed in this work are carried out with maximum PD of 14 MW/m^2 (13.5 MW/m^2 electrons PD plus 0.5 MW/m^2 ions PD) to examine load conditions satisfying the fatigue design criteria.

The applied PDs are conducted from the surface to the coolant and cause the temperature profile in the LEE’s material. The main model parameters are following introduced.

Table 1. Main design parameters for LEE thermo-hydraulic and thermo-mechanical analyses.

Description	Symbol	Value
Structural LEE material	CuCrZr-IG	-
Inner diameter of the tube	D_h [mm]	30
Minimum wall thickness	TK [mm]	2.5
LEE length	L_{LEE} [m]	1.7
Twist tape pitch	t_{tt} [mm]	60
Asymmetric PDs, maximum PD	PD_{max} [MW/m^2]	14.0
Water coolant flow-rate	$\dot{m}$ [kg/s]	4.0
Breakdown pause for transient thermo-hydraulic analyses [1]	t_{bd} [ms]	30
Inlet water bulk temperature	T_{inlet} [°C]	140
Outlet water bulk pressure	p_{outlet} [MPa]	0.85
Maximum admissible material temperature	T_{adm} [°C]	350
Required beam-on beam-off cycles	$N_{req\ beam\text{-}on/off}$	$5.0 \cdot 10^4$
Required breakdown cycles	$N_{req\ breakdowns}$	$4.5 \cdot 10^5$

Steady-state and transient thermo-hydraulic analyses are carried out considering the NBI operations applying a procedure for combination of cycles that returns beam-on beam-off and breakdown cycles [1, 16]. The results of the thermal analyses obtained at different instants are applied as body loads in the subsequent thermo-structural analyses by means of sequentially coupled physics analyses.

FE Model Description

The three dimensional solid model and the thermal-fluid pipe, are created with the bottom-up technique and dragging the lowest-order model entities along the LEE longitudinal direction [14]. More coordinate systems are defined with X and Y coordinates in the transverse section and Z as longitudinal axis. A fine mesh of solid elements with 2.5 mm height, 2 mm length, and 0.75 mm thickness (mean values in a transverse section) is modeled.

The element types and the applied loads and boundary conditions are shown in Figure 2.

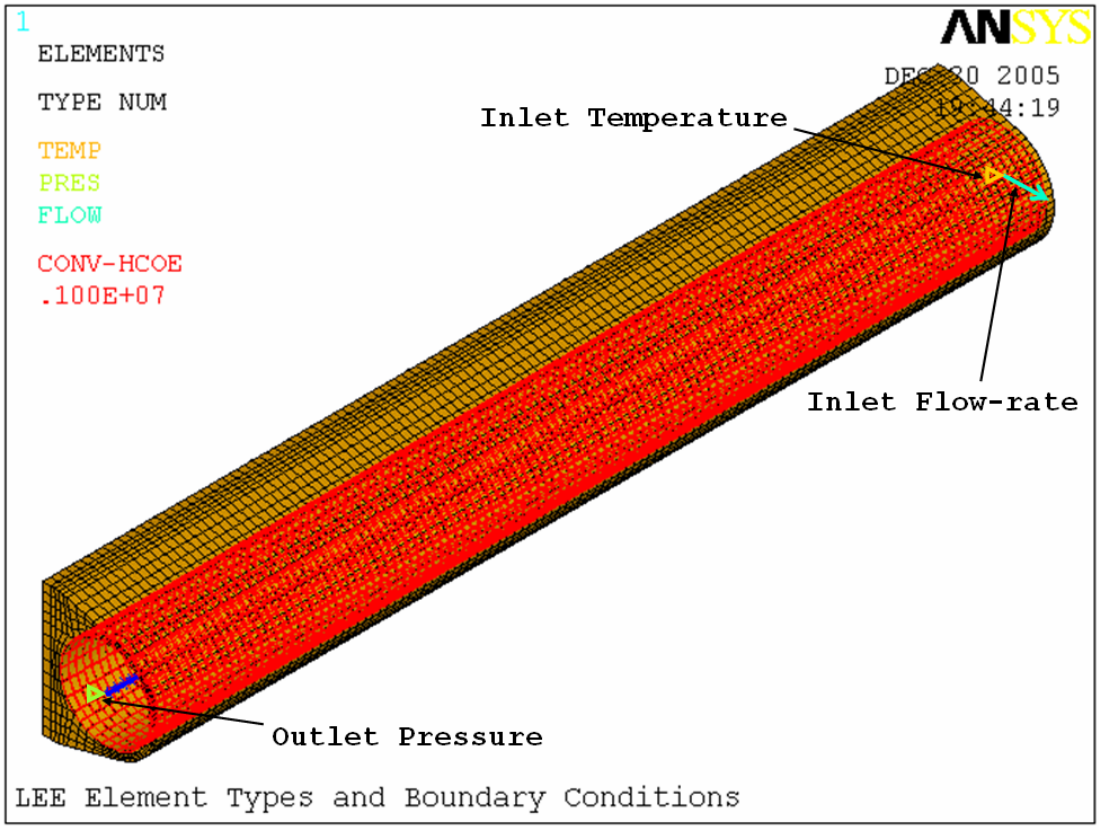

Figure 2. Element types of the neutralizer LEE model. ■: 3-D solid thermal/structural elements. ■: coupled thermal-fluid pipe elements. ■: 3-D thermal surface elements. The constant heat transfer coefficient assigned before the solution is displayed. The applied boundary conditions are the inlet coolant temperature, inlet flow-rate, and outlet pressure.

The element type "■" refers to solid thermal/structural elements (solid70/solid45) associated with the material describing the properties of copper alloy CuCrZr-IG [15]. This material has high thermal conductivity so that heat transfer out of the element can be accomplished as efficiently as possible. Its relatively low melting point limits the range of temperature over which it can be used (350 °C is the maximum admissible temperature). The material properties are function of temperature by means of coefficients for linear, quadratic, cubic, and quartic terms.

The element type "■" refers to coupled thermal-fluid pipe elements (fluid116) with temperature and pressure degrees of freedom, two nodes and convection information passed to thermal surface elements (surf152), friction factor being a function of temperature and Reynolds's number using data tables. The material associated with this element type is the water coolant [13]. Water properties versus temperature are plotted in form of polynomial functions.

The element type "■" refers to thermal surface elements (surf152) with midside nodes that match the adjacent solid elements: "surf152" are pasted onto the actual solid model. Each surface element has extra-node used as bulk temperature.

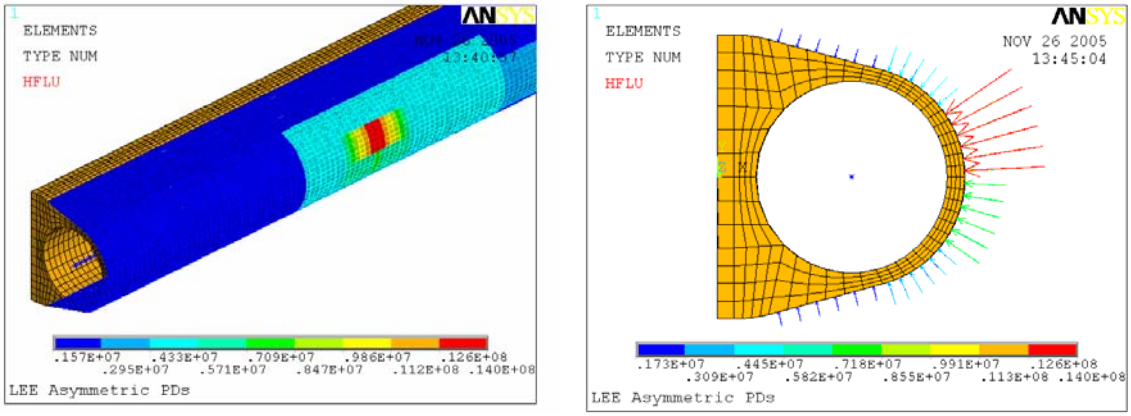

a) PDs showed as contours [W/m^2]. **b) PDs showed as arrows [W/m^2].**

Figure 3. Asymmetric PDs applied on the LEE.

FE Analyses

The results of the analyses are the temperature profiles in the LEE material, fluid dynamic parameters of the liquid bulk, and stresses and strains during beam-on beam-off and breakdown cycles.

The results of the thermo-hydraulic analyses are important for the following reasons:

- verify the operating thermal range of the material in the several load conditions;
- design the hydraulic circuit in all its parameters.

Also the thermal results in the considered time range are input data for the thermo-structural analyses. The next few topics describe convergence behavior during the iterations for nonlinear analyses. Subsequently the main results are presented.

Converged Solutions

The higher convergence instabilities occur solving the load step with full PDs applied on the LEE. The number of iterations to convergence is reduced mitigating the instabilities in the heat flux due to variations in nucleate boiling conditions in the near-wall surface elements. Three versions of the customized ANSYS code are examined. The first compiled and relinked with the customized routine that calls the damping function calculating the Geometric Mean of the inner wall temperature of each surface element (code GM), the second that calculates the Arithmetic Mean (code AM), and the last Without the Damping function (code WD).

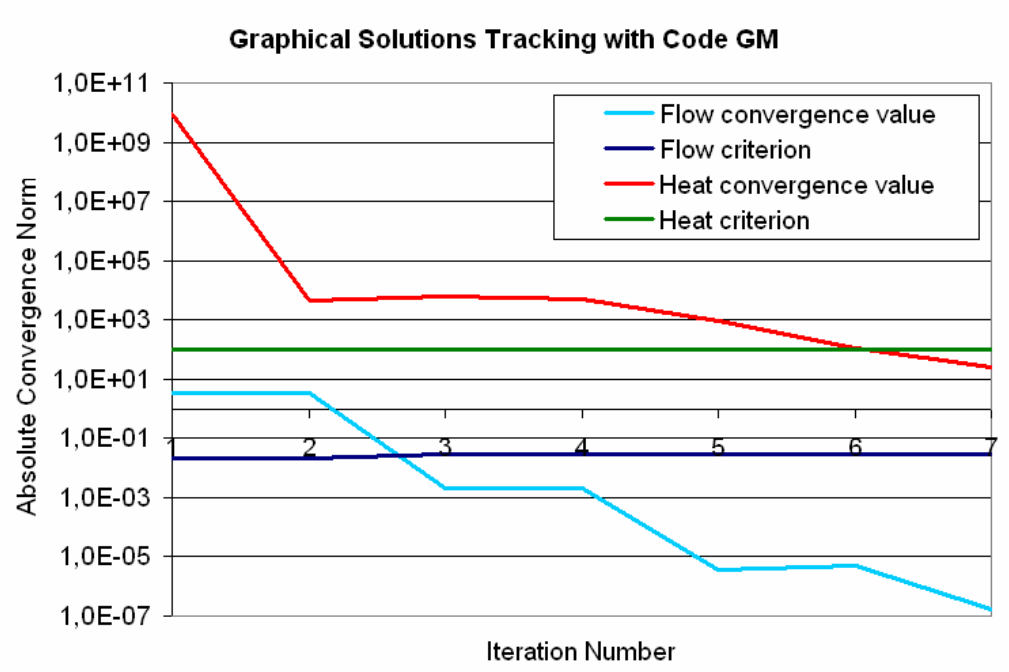

Figure 4. Graphical solutions tracking for nonlinear analysis solved with code GM. 7 iterations to convergence.

The benefit in number of iterations to convergence due to the damping functions is evident comparing the solutions tracking for the different versions of the customized ANSYS code. The heat flux convergence criterion is set to $10^2 = 10^4 \cdot 10^{-2}$ (typical value · tolerance about value with square root of sum of squares norm).

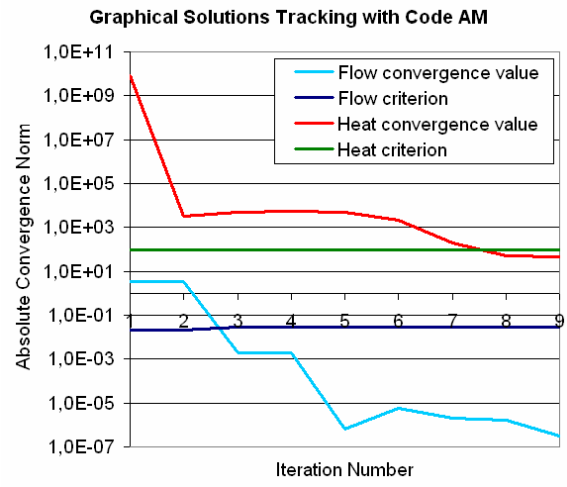

a) Code AM, 9 iterations to convergence.

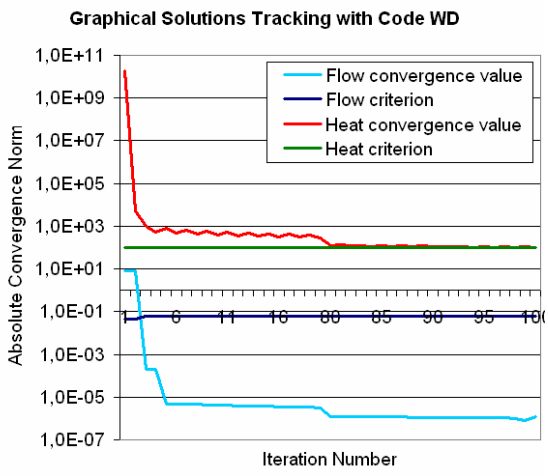

b) Code WD, 100 iterations to convergence.

Figure 5. Graphical solutions tracking for nonlinear analyses solved with customized codes AM and WD.

The code WD is not successful to reach convergence with the assigned coolant flow-rate $\dot{m} = 4.0\,kg/s$ that is necessary to exhaust the heat flux with 22/16 = 1.4 safety factor (CHF and maximum heat flux at the inner channel surface ratio). The heat flux variations between two subsequent iterations are reduced increasing the flow-rate to forbid the nucleate boiling phenomenon where the heat flux is insufficient to maintain the nucleate boiling conditions. The increased flow-rate restricts the nucleate boiling in the surface elements in steady-state conditions. The convergence is reached increasing the flow-rate up to $\dot{m} = 9.15\,kg/s$. The number of iterations to convergence is $i_{code\ WD} = 100$ with flow-rate $\dot{m} = 9.15\,kg/s$, $i_{code\ WD} = 152$ with flow-rate $\dot{m} = 9.1\,kg/s$, $i_{code\ WD}$ greater than 200 with flow-rate $\dot{m} = 9.0\,kg/s$.

FE Analyses Results

The main fluid dynamic results using the code GM are following tabulated.

Table 2. Main thermal and fluid dynamic results of the STE LEE thermo-hydraulic analyses.

Description	Symbol	Value
Inlet water bulk temperature	T_{inlet} [°C]	140
Outlet water bulk temperature	T_{outlet} [°C]	155
Inlet water bulk pressure	p_{inlet} [MPa]	1.0
Outlet water bulk pressure	p_{outlet} [MPa]	0.85
Flow velocity	v [m/s]	6.1
Flow Reynolds's number	Re	$8.7 \cdot 10^5$
Friction coefficient	f	0.11
CHF / maximum heat flux at the inner channel surface	F_{CHF} [(MW/m^2)/(MW/m^2)]	22/16
Water saturation temperature at outlet	$T_{s\ outlet}$ [°C]	171.2
Boiling start-up temperature	T_{si} [°C]	179
Boiling margin of safety	$\Delta T = T_{outlet} - T_{s\ outlet}$ [°C]	16.2

The boiling margin of safety represents the maximum further water temperature increase due to abnormal conditions. The mapping of heat fluxes and heat transfer coefficient versus the longitudinal coordinate or fluid node number are important to understand the activation of the heat transfer phenomena, but they are not in the aims of this work.

Thermo-hydraulic transient analyses are carried out during the time range of a breakdown. Transient PDs load starting from steady state at full PDs and the time independent solution is solved at instant $t_1 = 10^{-6}$ s applying the full PDs (load step 1). The PDs are stepped to zero (load step 2) up to instant $t_2 = 3.0 \cdot 10^{-2}$ s (no PDs for 30 ms breakdowns pause) and then the PDs are linearly interpolated up to full PDs in 80 ms (linear power ramp up to instant $t_3 = 11.0 \cdot 10^{-2}$ s).

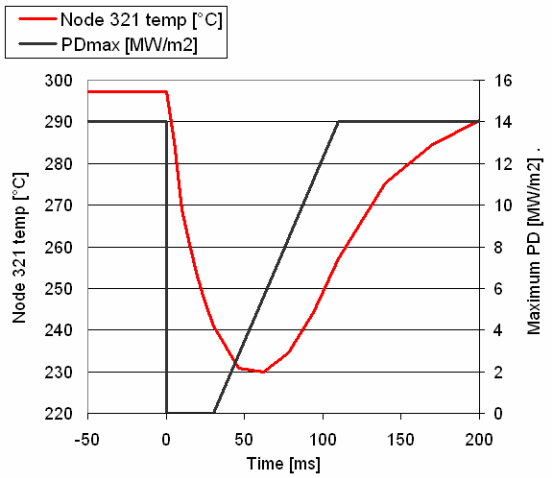

a) **Maximum PD and node temperature versus time during a breakdown.**

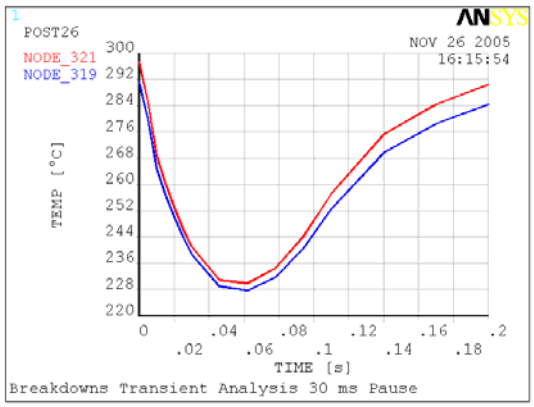

b) **Temperatures of nodes 321 and 319 versus time during a breakdown.**

Figure 6. Breakdowns transient analysis with 30 ms pause. Temperatures of the nodes 321 and 319 situated in the middle plane of LEE with Z_{321} = 0.695 m and Z_{319} = 0.690 m.

The contours of thermo-hydraulic results are represented in the following Figures 7 and 8.

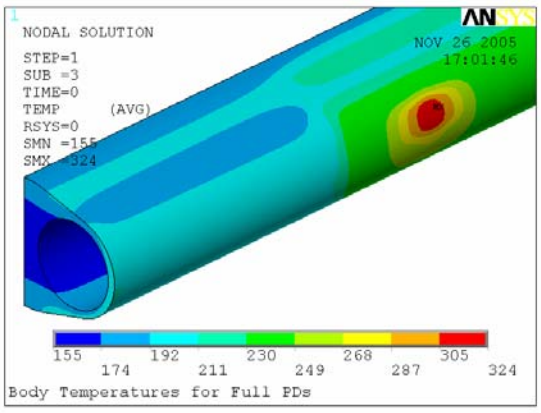

a) **Body temperatures of CuCrZr-IG [°C].**

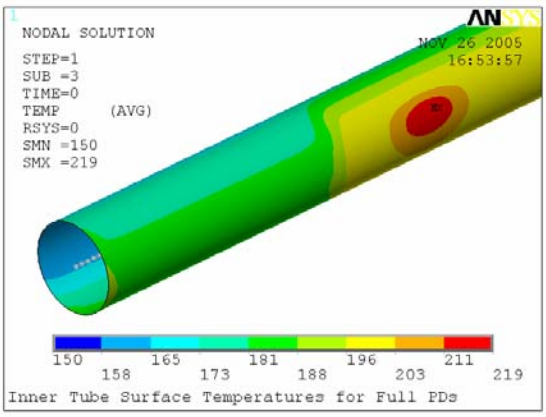

b) **Inner tube surface temperatures [°C].**

Figure 7. LEE temperature results in the region of 0.53 m ≤ Z ≤ 0.83 m for full PDs applied (load step 1).

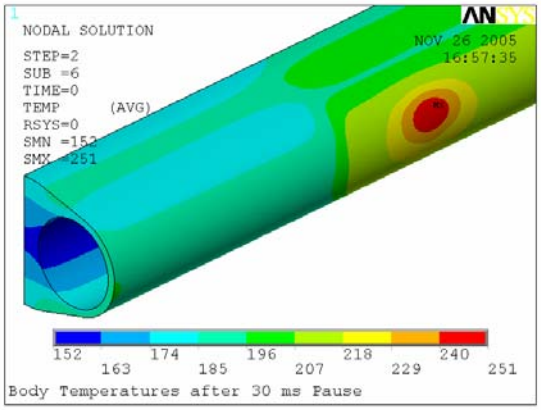

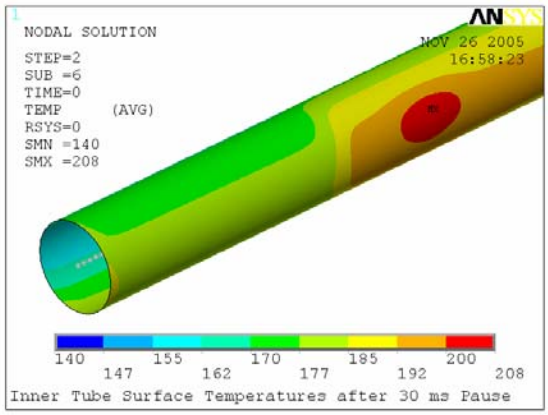

a) Body temperatures of CuCrZr-IG [°C]. **b) Inner tube surface temperatures [°C].**

Figure 8. LEE temperature results in the region of 0.53 m ≤ Z ≤ 0.83 m without PDs after 30 ms pause (load step 2).

The maximum material temperature is 324 °C that is less then the maximum admissible 350 °C. The main results of the thermo-structural analyses are presented in the following Figures 9 and 10.

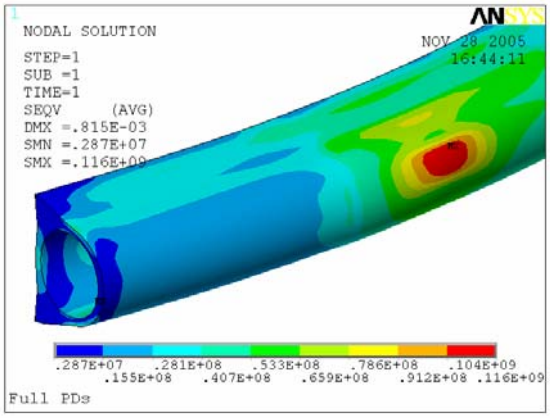

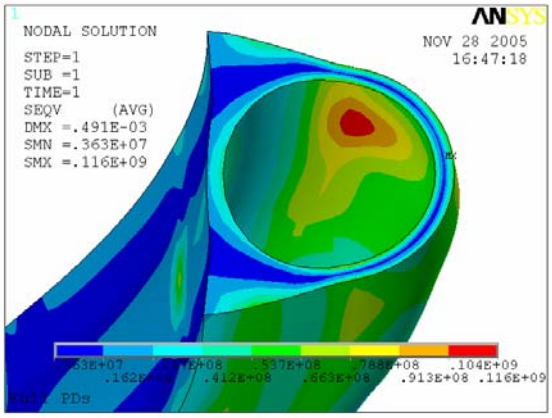

a) Compressive effect due to PDs. **b) Inner tube bending effect due to the thickness increase.**

Figure 9. LEE Equivalent Von Mises stresses [Pa] in the region of 0.53 m ≤ Z ≤ 0.83 m for full PDs applied (load step 1). Scale factor 100 for displacement amplitude.

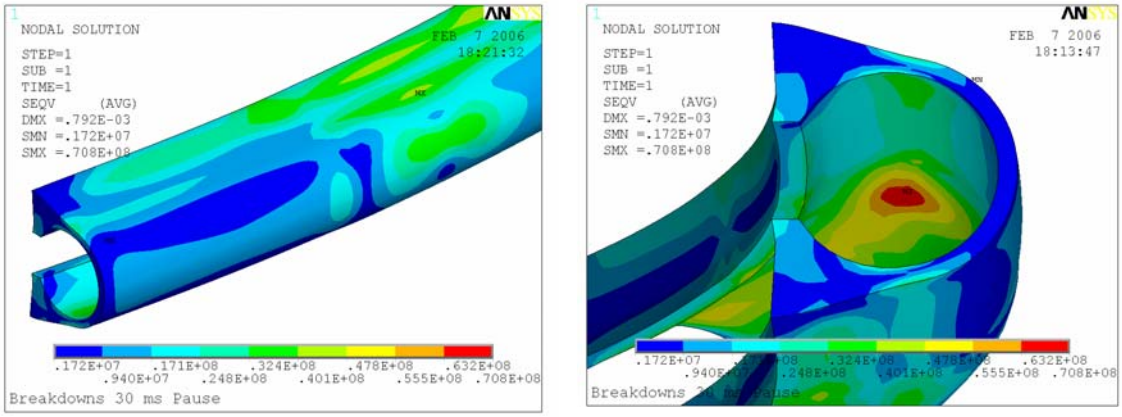

a) Compressive effect due to PDs.

b) Inner tube bending effect due to the thickness increase.

Figure 10. LEE Equivalent Von Mises stresses [Pa] in the region of 0.53 m ≤ Z ≤ 0.83 m without PDs after 30 ms pause (load step 2). Scale factor 100 for displacement amplitude.

After solved the elastic analyses, the rules of the applied code [18] require that the total stress be broken down into constituent parts, also known as stress categories. These stress categories, either alone or in various combinations, are compared with various limits in satisfying these criteria. It should be noted that, in all of these stress categories, the stress constituents are functions of position in the structure. The maximum value (at any position) of a combination of the constituents is compared against a limit.

The monotonic type (M-type) damage denotes damage in a structure which can result from the application of a steadily and regularly increasing loading, a constant loading, or the loading corresponding to the first quarter cycle of a cyclic load; the cyclic type (C-type) damage denotes damage that results from repeated application of loadings (ratcheting and fatigue). The criteria for prevention of M-type damages are satisfied. Stress and strain fields during beam-on beam-off and breakdown cycles are used to carry out the thermo-fatigue life assessment.

Thermo-fatigue Life Assessment

The results of thermo-structural analyses are post-processed applying the rules of criteria for damage verification [18, 19]. In this work only the results of the fatigue verifications are presented because they are the most critical for the required operating conditions.

The procedure for the fatigue life assessment is applied considering stress and strain fields during beam-on beam-off and breakdown cycles. The results of transient analyses in each node of the model are post-processed by means of a suitable macro developed in Visual Basic carrying out the thermo-fatigue life assessment.

The three-axial fatigue criterion of octahedral shear stress theory is applied with the material characteristic properties function of temperature. The principal strains in a node during the considered cyclic load (beam-on beam-off or breakdown) are combined to calculate the elastic equivalent strain range:

$$\Delta\varepsilon_{el} = \frac{1}{\sqrt{2}} \cdot \frac{1}{1+\nu} \cdot \left[\left(\Delta\varepsilon_1 - \Delta\varepsilon_2\right)^2 + \left(\Delta\varepsilon_2 - \Delta\varepsilon_3\right)^2 + \left(\Delta\varepsilon_3 - \Delta\varepsilon_1\right)^2 \right]^{1/2}$$

The elastic equivalent strain range is corrected due to the local effects of plasticity obtaining the equivalent strain range $\Delta\varepsilon_{eq}$ [15, 16].

The effects of the mean strain on the fatigue design curve are taken into account drawing the local Haigh diagram for each node [20]. The calculation of the equivalent mean strain in value and sign, and the construction of the Haigh diagram and the fatigue design curve in each node are left out because they are not in the aims of this work. The main results are represented in the following Figures 11, 12, 13, and Table 3.

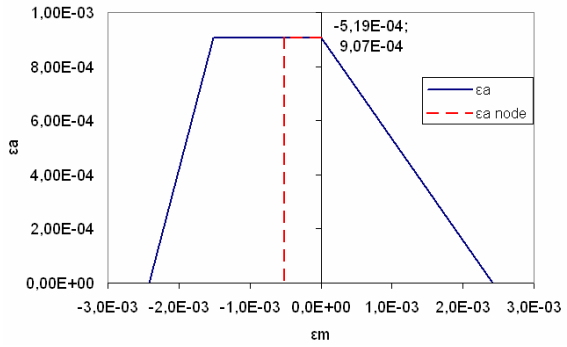

a) Haigh diagram for the effects of mean strain drawn for N = $1.25 \cdot 10^5$.

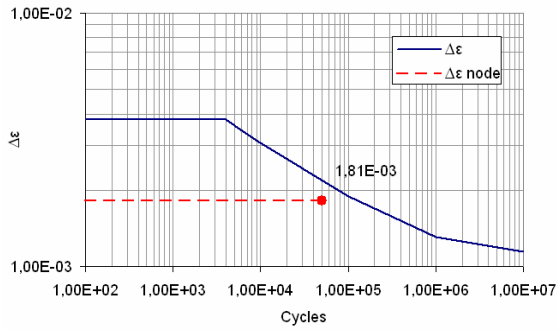

b) Fatigue design curve and fatigue life. Fatigue usage fraction $V_{beam\text{-}on/off}$ = $5.0 \cdot 10^4 / 1.25 \cdot 10^5$ = 40%.

Figure 11. Fatigue life assessment for beam-on beam-off cycles at the worst loaded node.

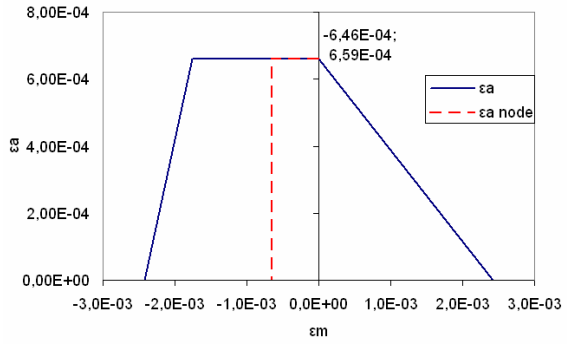

a) Haigh diagram for the effects of mean strain drawn for N = $9.16 \cdot 10^5$.

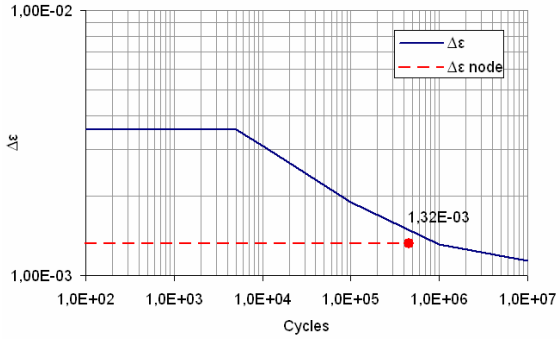

b) Fatigue design curve and fatigue life. Fatigue usage fraction $V_{breakdowns}$ = $4.5 \cdot 10^5 / 9.16 \cdot 10^5$ = 49%.

Figure 12. Fatigue life assessment for breakdown cycles at the worst loaded node.

Table 3. Main results of the fatigue life assessment (breakdowns pause 30 ms).

Parameter	Beam-on beam-off	Breakdowns
T_{node} [°C]	191.8	
$\Delta\sigma_{el}$ [MPa]	115	88
$\Delta\varepsilon_{eq}$	$1.81 \cdot 10^{-3}$	$1.32 \cdot 10^{-3}$
ε_m	$-5.19 \cdot 10^{-4}$	$-6.46 \cdot 10^{-4}$
N_{req} (cycles)	$5.0 \cdot 10^{4}$	$4.5 \cdot 10^{5}$
Fatigue life (cycles)	$1.25 \cdot 10^{5}$	$9.16 \cdot 10^{5}$
V_i [%]	40%	49%
Fatigue damage [%]	**89%**	

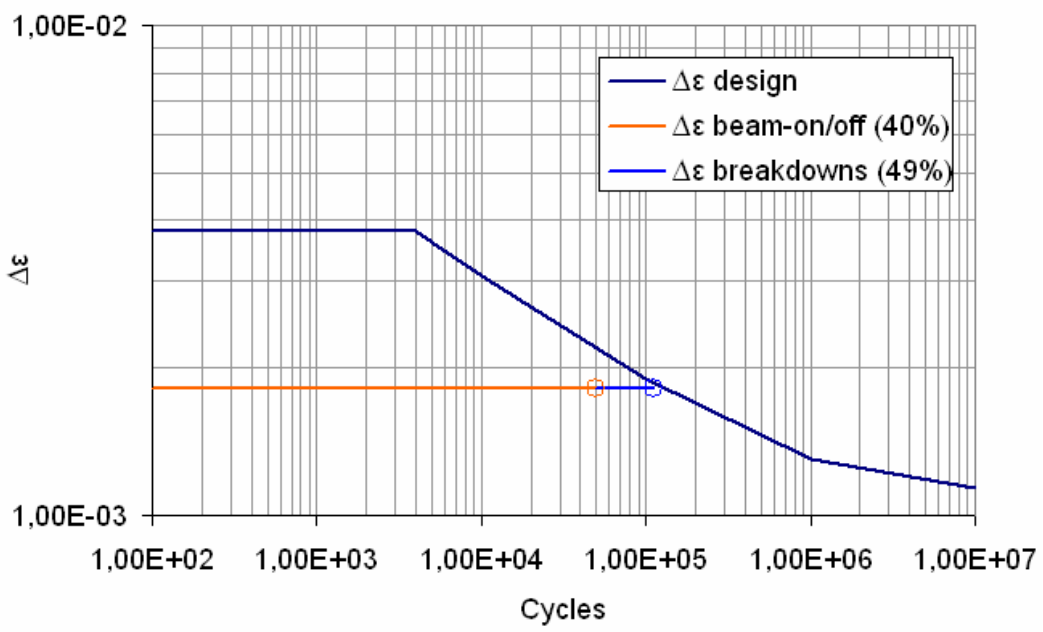

Figure 13. Fatigue damage of 89% for beam-on beam-off and breakdown cycles at the worst loaded node of the neutralizer LEE.

For each cyclic load the fatigue usage fraction (V_i) is calculated (Figures 11 and 12). The sum of the fatigue usage fractions for all cyclic loads and in each node is the fatigue damage of that node. The worst loaded nodes (Figure 13) are located in the frontal surface exposed to the beam (compressive load).

Conclusions

The customized ANSYS code allows us to carry out coupled thermo-hydraulic and thermo-mechanical analyses of high heat flux components with swirl tube elements.

The damping function implemented in the user programmable routine, so named because it reduces the fluctuation in heat flux between iteration and the previous one, allows to diminish at least one order of magnitude the number of iteration to convergence with reduced time of analysis. Furthermore, the damping function is necessary to reach convergence solutions in the analysis where nucleate boiling conditions are foreseen in extended areas of the model. The only possibility to reach convergence in these analyses with the assigned thermal loads and without using the damping function, is to increase the flow-rate to forbid the nucleate boiling phenomenon where the heat flux is insufficient to maintain the nucleate boiling conditions. In this way the increased flow-rate reduces the heat flux instabilities but it can be really improbable and the number of iterations to convergence becomes very high.

The customized routine compiled and re-linked in the ANSYS code is a general tool applicable to high heat flux components in fusion technology. Dedicated neural networks that simulate heat exchange in swirl tube elements or other devices as hypervapotrons, are possible reliable models that can be implemented in the ANSYS customized code.

The results of coupled thermo-hydraulic and thermo-mechanical analyses of the ITER neutralizer centre leading edge using the customized ANSYS code are explained in this work. After solved the elastic analyses, the rules of the applied design criteria require that the total stress be broken down into stress categories.

The procedure for the fatigue life assessment is applied considering stress and strain fields during beam-on beam-off and breakdown cycles. The results of transient analyses in each node of the model are post-processed by means of a suitable macro, developed in Visual Basic, carrying out the thermo-fatigue life assessment: the three-axial fatigue criterion of octahedral shear stress theory is applied with the material characteristic properties function of temperature, the elastic equivalent strain range is corrected due to the local effects of plasticity in each node, the effects of the mean strain on the fatigue design curve are taken into account drawing the local Haigh diagram in each node, the fatigue damage of each node is calculated as sum of the fatigue usage fractions of that node.

The criteria for prevention of damages which can result from the application of constant loads on the leading edge are satisfied, the maximum nodes temperature (324 °C) is less than the admissible (350 °C), and the thermo-fatigue verification is satisfied with 89% fatigue damage due to beam-on beam-off and breakdown cycles.

References

1 ITER DDD5.3 Appendix 4, Thermohydraulic and Thermomechanical Analyses of the High Heat Flux Beam Line Components, N 53 DDD 33 01-07-10 R 0.1.

2 ITER DDD5.3, Neutral Beam Heating and Current Drive (NBH&CD) System, N 53 DDD 29 01-07-03 R 0.1.

3 Naumov V.K., Semashko N.N., Analytical Model for Estimating Thermophysical and Strength Parameters of the Cooled Pipe with the Twisted Tape under Asymmetric Heating by a Pulse of External Heat Flux, Plasma Devices and Operations, 1994, vol. 3, pp. 267-280.

4 Naumov V.K., Semashko N.N., Finite-difference Approximation of the Adiabatic Cross-section Technique in a Numerical Analysis of the Single-side Heating Process of a Cooled Pipe with the Twisted Tape Inside by an External Heat Flux Pulse, Plasma Devices and Operations, 1995, vol. 4, pp. 141-161.

5 Lopina R.F., Bergles A.E., Heat Transfer and Pressure Drop in Tape-Generated Swirl Flow of Single-Phase Water, Transaction of the ASME, Journal of Heat Transfer, August 1969, pp. 434-445.

6 Naumov V.K. et.al., Method of Adiabatic Cross-section and its Application for Estimating of Thermophysical and Thermostrength Parameters of High Density Beam Dumps in the ITER Injection System, Plasma Devices and Operations, 1999, vol. 8, pp. 39-65.

7 Thom J.R.S., Walter W.M., Fallon T.A., Reising G.F.S., Symposium on Boiling Heat Transfer in Steam Generating Units and Heat Exchangers, Manchester, 15-16 September 1965.

8 Kutateladze S.S., Fundamental Heat Exchange Theory, 5th edd., suppl. Atomizdat, Moscow, 1979.

9 Yagov V.V., Zudin Yu.B., Proceeding 10th International Heat Transfer Conference, 1994, vol. 5, pp. 189-194.

10 EU Home Team, Final Report on Task PDT 2-4, Thermal hydraulic test on divertor targets using swirl tubes, CEA (Schlosser J., Boscary J.).

11 John H. Lienhard, A Heat Transfer Handbook Third Edition, Cambridge Massachusetts, January 2004.

12 Bergles A.E, Rohsenow W.M., Paper 63-HT-22, 6th National Heat Transfer Conference of the ASME-AIChE, Boston, 11-14 August 1963.

13 SteamTab™ add-in software, Implementation of steam properties formulation approved by the International Association for the Properties of Water and Steam (IAPWS): The IAPWS Formulation of Ordinary Water for General and Scientific Use (IAPWS-95).

14 ANSYS Release 8.0 Documentation, Element Reference, Element Library.

15 ITER SDC-IC Appendix A, Materials Design Limit Data, G 74 MA 8 R0.1, July 2004.

16 ITER SDC-IC Appendix B, Guidelines for Analysis, In-vessel Components, G 74 MA 8 R0.1.

17 H.P.L. de Esch, ITER-SINGAP Full Geometry Simulations, June 2003 (CCNB meeting).

18 ITER SDC-IC, Structural Design Criteria for ITER In-Vessel Components, July 2004.

19 Criteria of the ASME Boiler and Pressure Vessel Code for Design by Analysis in Sections III and VIII, Division 2, The American Society of Mechanical Engineers, United Engineering Center, New York.

20 Papadopoulos I.V., Davoli P., Gorla C., Filippini M., Bernasconi A., A comparative study of multiaxial high-cycle fatigue criteria for metals, International Journal of Fatigue, Vol. 19, Issue 3, March 1997, pp. 219-235.

Acknowledgment

This work, supported by the European Communities under the contract of Association between EURATOM-ENEA, was carried out within the framework of the European Fusion Development Agreement. The views and opinions expressed herein do not necessarily reflect those of the European Commission.